

Structure and microwave dielectric properties of $\text{Ba}_{1+x}[(\text{Co}_{0.7}\text{Zn}_{0.3})_{1/3}\text{Nb}_{2/3}]\text{O}_3$ ($-0.015 \leq x \leq 0.015$)

J.J. Bian*, G.X. Song, K. Yan

Department of Inorganic Materials, Shanghai University, 149 Yanchang Road, Shanghai 200072, China

Available online 13 December 2006

Abstract

The sintering behavior, ordering state and microwave dielectric properties of $\text{Ba}_{1+x}(\text{Zn}_{0.3}\text{Co}_{0.7})_{1/3}\text{Nb}_{2/3}$ Ceramics ($-0.015 \leq x \leq 0.015$) were investigated in this paper. The X-ray diffraction (XRD) results show that all samples exhibit a single phase except for the sample with $x = -0.015$. Scanning electron microscopy (SEM) observation and energy dispersion analysis (EDS) indicate that the second phase is barium niobate. Raman spectrum reveal the presence of long range order (LRO) of B-site ions when $-0.015 \leq x < 0$ and only short range order (SRO) when $0 \leq x \leq 0.015$. The sinterability is decreased for the samples with $x > 0$. The dielectric constant slightly decreases when $x < 0$ and decreases greatly when $x > 0$. The $Q \times f$ value of the samples with $x > 0$ is much lower than that with $x < 0$. The maximum $Q \times f$ value of 70,917 GHz is obtained when $x = -0.01$. The temperature coefficient of resonant frequency exhibits positive value for the samples with $x \geq 0$ and negative value for the samples with $x < 0$. Near zero temperature coefficient of resonant frequency was obtained when $x = 0.002$.

© 2006 Elsevier Ltd. All rights reserved.

Keyword: Nonstoichiometric

1. Introduction

With the development of wireless communication, especially the third generation telecommunication (3G), low cost microwave dielectrics with high Q factor are desired. Requirements for these dielectric materials must be the combined microwave dielectric properties of high dielectric constant ($\epsilon_r > 30$), high unload quality factor ($Q \times f > 40,000$ GHz) and a temperature coefficient of the resonant frequency (τ_f) tunable through zero. Recently dielectric resonators of Nb-based compounds with a complex perovskite structure have been extensively studied due to their very high quality factor in microwave frequency and relative low cost compared with Ta-based complex perovskite ceramics.^{1–4} Among these materials, $\text{Ba}(\text{Co}_{0.7}\text{Zn}_{0.3})_{1/3}\text{Nb}_{2/3}\text{O}_3$ (BCZN) has been reported to possess high dielectric constant ($\epsilon_r \sim 34.5$), a high Q value ($Q \times f = 56,000$ – $97,000$ GHz) and small temperature coefficient of resonant frequency ($\tau_f \sim 0$).³ However, its Q value is very sensitive to processing conditions. The poor reproducibility of Q values was considered to be related to the difficult control of the B-site ordering degree and valence state of Co.²

The effect of B-site doping on the structure, sinterability and microwave dielectric properties of BCZN have been investigated by Azough et al.^{5–6} It is well established that the Q values of complex perovskite ceramics increase with the increase of B-site cation ordering degree. It was reported that the B-site ordering degree of $\text{Ba}(\text{Mg}_{1/3}\text{Ta}_{2/3})\text{O}_3$ (BMT) and $\text{Ba}(\text{Zn}_{1/3}\text{Nb}_{2/3})\text{O}_3$ (BZN) was enhanced by the introduction of small amount of A-site deficiency.^{7,8}

In this research paper, the effect of A-site nonstoichiometry on the densification, microstructure, structural ordering, and microwave dielectric properties of $\text{Ba}(\text{Co}_{0.7}\text{Zn}_{0.3})_{1/3}\text{Nb}_{2/3}\text{O}_3$ is investigated.

2. Experiment

$\text{Ba}_{1+x}[(\text{Co}_{0.7}\text{Zn}_{0.3})_{1/3}\text{Nb}_{2/3}]\text{O}_3$ ($-0.015 \leq x \leq 0.015$) ceramic samples were prepared by conventional solid-state reaction process from the starting materials including Nb_2O_5 (99.9%), CoO (99.8%), BaCO_3 (99.7%, impurities of Ca^{2+} and Sr^{2+} are less than 0.15 wt.%) and ZnO (99.6%). The $\text{Ba}_{1+x}[(\text{Co}_{0.7}\text{Zn}_{0.3})_{1/3}\text{Nb}_{2/3}]\text{O}_3$ ($-0.015 \leq x \leq 0.015$) compounds were weighed and mixed with ZrO_2 balls in ethanol for 24 h, dried and calcined at the temperature of 1150 °C for 2 h in a alumina crucible. The calcined powders were grounded, dried and mixed with 7 wt.% PVA. The mixtures were pressed into

* Corresponding author. Tel.: +86 21 56331697; fax: +86 21 56332694.
E-mail address: jjbian1@sohu.com (J.J. Bian).

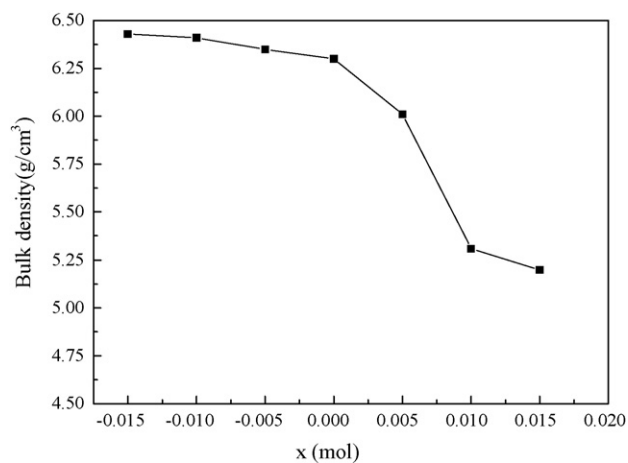


Fig. 1. Variation of bulk density of samples sintered at 1450 °C/10 h as function of x value.

pellets. The compacts were sintered between 1450 °C for 10 h. In order to prevent the Co and Zn evaporation loss, the compacts were muffled with powder of the same composition. A cooling rate of 100 °C/h was employed.

The phase constitutes of the sintered samples were identified by X-ray powder diffraction (XRD) with Ni-filtered Cu K α radiation (40 kV and 20 mA, Model Dmax-RC, Japan). In order to avoid the influence of the second phases formed on the surface during sintering, the surface of the specimen for XRD was abraded. Powder diffraction patterns were taken for $60^\circ < 2\theta < 140^\circ$ with 0.01° step scanning for precise lattice parameter measurement. Silicon powders were mixed as an internal standard. Bulk density of the sintered specimens

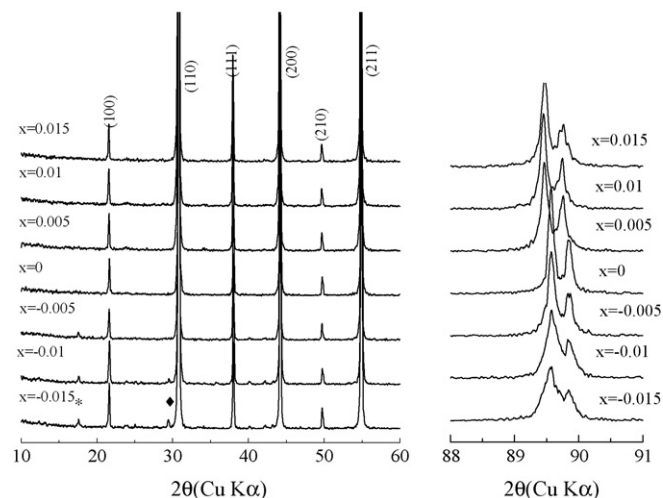


Fig. 2. XRD patterns of the sintered specimens with different x value: (*, superlattice reflection caused by B-site ordering; ♦, reflection caused by second phase).

was identified by Archimedes' method. The Raman experiments were carried out for the sintered samples (Model Jobin Y'von U1000). A laser line of 532 nm and 500 mW average power was used. The spectra were recorded from 0 to 1000 cm^{-1} . The microstructure of the sintered sample was characterized by scanning electron microscopy (SEM) (Model XL20, Philips Instruments, Netherlands). All samples were polished and thermal etched at the temperature which was 200 °C lower than its sintering temperature. Microwave dielectric properties of the sintered samples were measured between 7 and 8 GHz using network analyzer (Hewlett Packard, Model HP8720C, USA). The

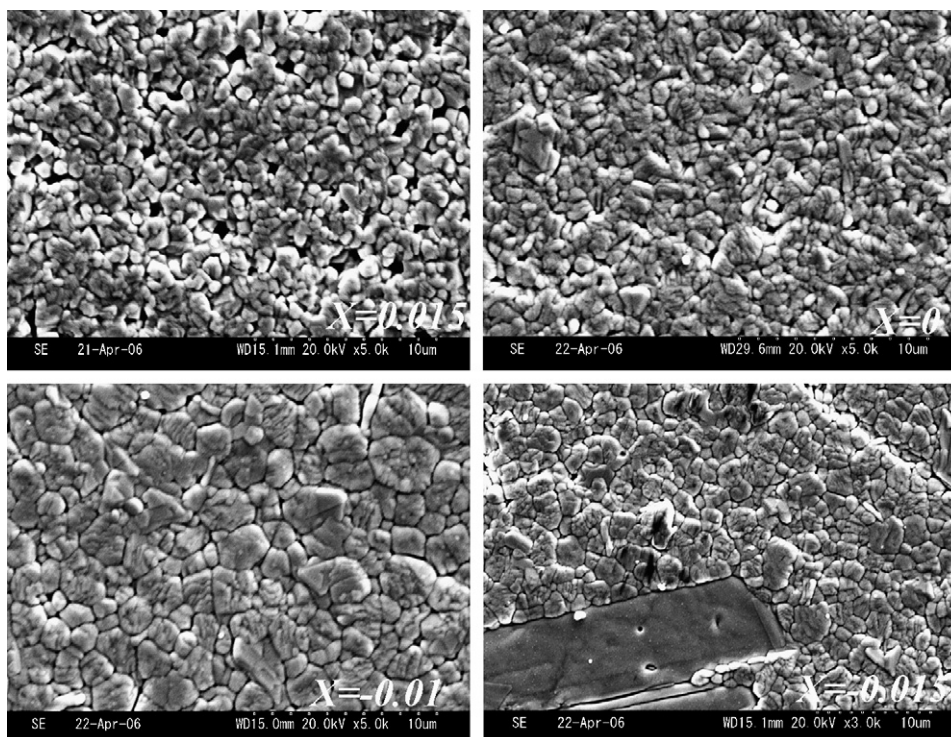


Fig. 3. SEM photographs of specimens with different x value sintered at 1450 °C/10 h.

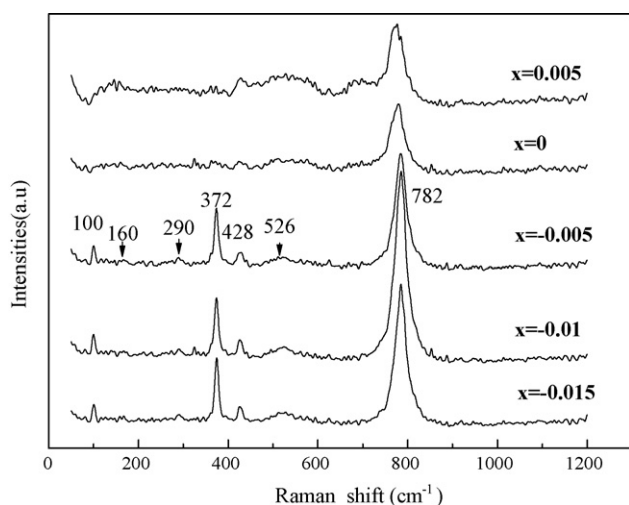


Fig. 4. Raman spectrum of the sintered specimens with different x value.

quality factor was measured by the transmission cavity method. The relative dielectric constant (ϵ_r) was measured according to the Hakki–Coleman method using the TE_{011} resonant mode, and the temperature coefficient of the resonator frequency (τ_f) was measured using invar cavity in the temperature range from 20 to 80 °C.

3. Results and discussions

Fig. 1 shows the variation of bulk density of specimens sintered at 1450 °C/10 h as function of x value. The bulk density varies slightly when $x \leq 0$, and decrease greatly with the

increase of x value when $x > 0$. The specimens with $x > 0$ show poor densification compared with the specimens with $x \leq 0$. The improvement of sinterability for the specimens with $x < 0$ is related to high bulk diffusion due to vacancies created by Ba-deficiency. This result is consistent with the similar observations made in BMT.⁵ Fig. 2 shows the XRD patterns of the sintered specimens with different x value. All the peaks were indexed according to a simple perovskite cell. No second phase was detected within the limits of experimental error except for the sample with $x = -0.015$. The Ba-deficient samples exhibit small weak superlattice reflection marked by star symbol. In addition it is noted that the reflection peaks shift to lower degree for Ba-excessive specimens compared with the samples with $x \leq 0$. It indicates increase of unit-cell volume for the Ba-excessive specimens, which is agreement with the results of $Ba_{1+x}(Zn_{1/3}Nb_{2/3})O_3$ reported by Davies.⁸ The expansion of the unit-cell for Ba-excessive specimens was considered to be caused by the partial substitution of the larger Ba cation onto the B-site.⁸ Fig. 3 shows the typical SEM photographs of samples with $x = 0, 0.015, -0.01$ and -0.015 sintered at 1450 °C/10 h. The microstructure of Ba-deficient specimen is denser than that of Ba-excessive specimens, which is agreement with the bulk density data presented in Fig. 1. The grain size of Ba-deficient specimen is larger than that of the Ba-excessive specimens, which is consistent with the XRD patterns exhibiting weak and wide peak for Ba-excessive specimens. The excessive Ba would remain in the grain boundary as BaO and hinder grain boundary migration. For the sample with $x = -0.015$, a plate like second phase exists, which is identified as barium niobate compound by EDS analysis.



Fig. 5. $(1\ 1\ 0)_p$ zone axis SAD pattern obtained from grains in the sintered specimen with $x = -0.01$ (diffraction spots at the $\{h \pm 1/3, k \pm 1/3, l \pm 1/3\}$ position arises from the 1:2 LRO on B-site).

Raman spectroscopy was considered to be an ideal tool for probing the degree of cation ordering.⁹ For an ideal simple cubic structure, there is no Raman active mode in the first order vibrational spectrum. The existence of ordered regions with particular symmetry allows additional Raman scattering. 1:1 ordered perovskites with the $Fm3m$ symmetry allow four Raman active modes ($A_{1g} + E_g + 2F_g$), and 1:2 ordered perovskites with $P3m1$ symmetry allow nine Raman active modes ($4A_{1g} + 5E_g$).¹⁰ Each of the F_{2g} modes in an $Fm3m$ structure (1:1 compounds) splits into a doublet $A_{1g} + E_g$ in a $P3m1$ structure (1:2 compounds).⁹ Fig. 4 presents the Raman spectroscopy of the sample with different x values. As can be seen, four intense and three weak lines can be observed in Ba-deficient samples, and only two lines can be observed in stoichiometric and Ba-excessive samples. The spectrum of Ba-deficient samples is similar to the spectrum of BCZN-BGT reported by Reaney et al.¹¹ The lowest band at 100 cm^{-1} corresponds to the motion of Ba ions against oxygen octahedral. The band at 430 cm^{-1} is associated with internal vibration of oxygen octahedral. The bands near 782 and 372 cm^{-1} are characteristic of ordering in B-site complex perovskites. The band at 372 cm^{-1} is only sensitive to long-range order (LRO) on the B-site whereas the band at 782 cm^{-1} ($A_{1g}(\text{O})$) may result from either LRO or short-range order (SRO).⁹ Narrow and intense peaks are usually observed for well-ordered structures, and generally sharpness and intensity of the Raman lines may be taken as a measure of the degree of ordering. Fig. 4 reveals that the Ba-deficient samples exhibit LRO and the degree of LRO increases up to $x = -0.01$ and slightly decreases with the further increase of Ba-deficiency. The LRO disappears and only SRO exists in stoichiometric and Ba-excessive samples. The increased LRO in Ba-deficient samples might result from the barium defects in crystalline to enhance the movement of cations. Slight decrease of LRO for the sample with $x = -0.015$ may be caused by the presence of barium niobate second phase as shown in Fig. 3. It is noted that the shift to higher frequency of $A_{1g}(\text{O})$ band (782 cm^{-1}) can be observed in Ba-deficient samples. The frequency of this band is mainly affected by the strength of B–O bonds (B: Nb, Zn and Co). As discussed above, the Ba vacancy will expand due to charge imbalance, which results in the compactness of oxygen

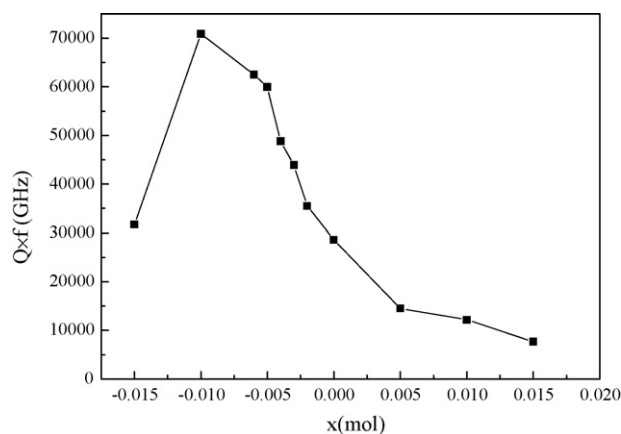


Fig. 7. Variation of $Q \times f$ value as function of x value.

octahedron and hence the bond strength of B–O is increased. Fig. 5 shows the $\langle 110 \rangle_p$ zone axis SAD pattern obtained from the grains in the sintered sample with $x = -0.01$. The presence of diffraction spots at the $\{h \pm 1/3, k \pm 1/3, l \pm 1/3\}$ position indicates the existence of 1:2 LRO in the sample with $x = -0.01$.

Fig. 6 shows the variation of dielectric constant as function of x value. The dielectric constant decrease slightly with the increase of Ba-deficiency, and decrease greatly with the increase of Ba-excess. The low permittivities of the Ba-excessive samples are mainly caused by their low bulk density. Fig. 7 shows the variation of $Q \times f$ value as function of x value. The $Q \times f$ value increases up to $x = -0.01$ and decreases with the further increase of barium deficiency. The improvement of $Q \times f$ value of barium-deficient samples is mainly due to the increase of LRO degree. The decrease of $Q \times f$ value for the sample with $x = -0.015$ is mainly caused by the presence of barium niobate second phase. For the samples with $x \geq 0$, although present only SRO and no big variation with x value, their $Q \times f$ values decrease with the increase of x value, which is mainly related to the decrease of bulk density with the increase of x value. Fig. 8 shows the variation of temperature coefficient of resonant frequency (τ_f) as function of x value. The absolute value of τ_f

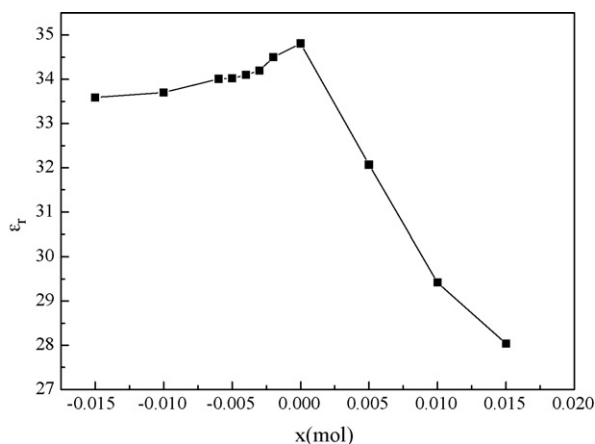


Fig. 6. Variation of dielectric constant as function of x value.

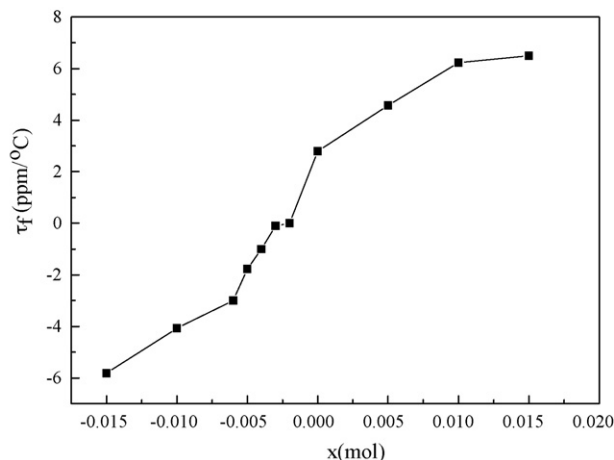


Fig. 8. Variation of temperature coefficient of resonant frequency as function of x value.

increases with the increase of barium nonstoichiometry. τ_f is negative when $-0.015 \leq x < 0$ and changed into positive value when $0 \leq x \leq 0.015$.

4. Conclusions

The effects of A-site nonstoichiometry on the sintering behavior, microstructure and microwave dielectric properties of BZCN have been studied in this paper. Ba-deficiency improves and Ba-excess retards the sinterability of BZCN, respectively. The LRO on B-site is greatly increased by slight Ba-deficiency on A-site ($-0.01 \leq x < 0$). Further increase of Ba-deficiency ($x = -0.015$) results in slightly decrease of 1:2 LRO degree due to appearance of barium niobate second phase. The stoichiometric and Ba-excessive samples exhibit only SRO on B-site. The $Q \times f$ value at microwave frequency is also greatly increased by slight Ba-deficiency due to the improvement of 1:2 LRO degree. The absolute value of τ_f increases with the increase of barium nonstoichiometry. τ_f is negative when $-0.015 \leq x < 0$ and changed into positive value when $0 \leq x \leq 0.015$. Good combination microwave dielectric properties were obtained for the sample with $x = -0.01$: $\varepsilon_r = 33.7$, $Q \times f = 70917$ GHz and $\tau_f = -4.07$ ppm/°C.

Acknowledgements

This work was supported by the Natural Science Foundation of China (NSFC) (project number: 50572060), Key founding for basic research of shanghai science and technology committee (06JC14070) and Sponsored by Shanghai Pujiang Program (D).

References

1. Scott, R. I., Thomas, M. and Hampson, C., Development of low cost, high performance $\text{Ba}(\text{Zn}_{1/3}\text{Nb}_{2/3})\text{O}_3$ based materials for microwave resonator applications. *J. Eur. Ceram. Soc.*, 2003, **23**, 2467–2471.
2. Endo, K., Fujimoto, K. and Murakawa, K., Dielectric properties of ceramics in $\text{Ba}(\text{Co}_{1/3}\text{Nb}_{2/3})\text{O}_3$ – $\text{Ba}(\text{Zn}_{1/3}\text{Nb}_{2/3})\text{O}_3$ solid solutions. *J. Am. Ceram. Soc.*, 1987, **70**(9), 215–218.
3. Ahn, C.-W., Jang, H.-J., Nahm, S., Park, H.-M. and Lee, H.-J., Effect of microstructure on the microwave dielectric properties of $\text{Ba}(\text{Co}_{1/3}\text{Nb}_{2/3})\text{O}_3$ and $(1-x)\text{Ba}(\text{Co}_{1/3}\text{Nb}_{2/3})\text{O}_3 + x\text{Ba}(\text{Zn}_{1/3}\text{Nb}_{2/3})\text{O}_3$ solid solutions. *J. Eur. Ceram. Soc.*, 2003, **23**, 2473–2478.
4. Hughes, H. and Iddles, D. M., Niobate-based microwave dielectrics suitable for third generation mobile phone base stations. *Appl. Phys. Lett.*, 2001, **79**(18), 2952–2954.
5. Azough, F., Leach, C. and Freer, R., Effect of CeO_2 on the sintering behaviour, cation order and properties of $\text{Ba}_3\text{Co}_{0.7}\text{Zn}_{0.3}\text{Nb}_2\text{O}_9$ ceramics. *J. Eur. Ceram. Soc.*, 2006, **26**, 1883–1887.
6. Azough, F., Leach, C. and Freer, R., Effect of V_2O_5 on the sintering behaviour, cation order and properties of $\text{Ba}_3\text{Co}_{0.7}\text{Zn}_{0.3}\text{Nb}_2\text{O}_9$ ceramics. *J. Eur. Ceram. Soc.*, 2005, **25**, 2839–2841.
7. Surendran, K. P., Sebastian, M. T., Mohanan, P., Moreira, R. L. and Dias, A., Effect of nonstoichiometry on the structure and microwave dielectric properties of $\text{Ba}(\text{Mg}_{0.33}\text{Ta}_{0.67})\text{O}_3$. *Chem. Mater.*, 2005, **17**, 142–151.
8. Wu, H. and Davies, P. K., Influence of non-stoichiometry on the structure and properties of $\text{Ba}(\text{Zn}_{1/3}\text{Nb}_{2/3})\text{O}_3$ microwave dielectrics: II. Compositional variations in pure BZN. *J. Am. Ceram. Soc.*, 2006, **89**(7), 2250–2263.
9. Zheng, H., Reaney, I. M., Csete de Gyorgfalva, G. D. C., Ubbelohde, R., Yarwood, J., Seabra, M. P. et al., Raman spectroscopy of CaTiO_3 -based perovskite solid solution. *J. Mater. Res.*, 2004, **19**(2), 488–495.
10. Siny, I. G., Tao, R., Katiyar, R. S., Guo, R. Y. and Bhalla, A. S., Raman spectroscopy of Mg-Ta order-disorder in $\text{Ba}(\text{Mg}_{1/3}\text{Ta}_{2/3})\text{O}_3$. *J. Phys. Chem. Solids*, 1998, **59**(2), 181–195.
11. Reaney, I. M., Iqbal, Y., Zheng, H., Feteira, A., Hughes, H., Iddles, D. et al., Order-disorder behaviour in $0.9\text{Ba}([\text{Zn}_{0.60}\text{Co}_{0.40}]_{1/3}\text{Nb}_{2/3})\text{O}_3$ – $0.1\text{Ba}(\text{Ga}_{0.5}\text{Ta}_{0.5})\text{O}_3$ microwave dielectric resonators. *J. Eur. Ceram. Soc.*, 2005, **25**, 1183–1189.